https://doi.org/10.46813/2025-155-046

NON-SELF-SUSTAINED ARC DISCHARGE IN MAGNETIC FIELD: INFLUENCE OF ADDITIONAL DISCHARGE IN E×B FIELDS ON THE MAIN CHARACTERISTICS OF THE ARC DISCHARGE IN ZIRCONIUM VAPOR AND THE PARAMETERS OF THE GENERATED PLASMA FLOWS

A.G. Borisenko

Institute for Nuclear Research NAS of Ukraine, Kyiv, Ukraine

E-mail: 2586864@ukr.net; boris@kinr.kiev.ua

The article presents the results of study of the non-self-sustained arc discharge with a magnetic field in zirconium vapors and the additional non-self-sustained discharge in E×B fields. Their main characteristics are given. The effect of the additional discharge on the electron temperature, plasma electron density, plasma potential and floating potential in the generated plasma flows of zirconium vapors is shown. It is established that even at low electric power, the additional discharge is able to double the density of plasma electrons in the flows. It is established that the anode potential drop in the arc discharge has a positive value over the entire range of discharge currents and decreases with its increasing. It is shown that the arc discharge in the anode material vapors is capable to generating plasma streams of zirconium vapors with the ionization coefficient from 60 to 90%. It has been established that the additional discharge in E×B fields is capable of increasing the ions fraction in the flows from 75 to 100% even at low arc discharge currents and can be used for the targeted regulation of ion fraction without changing the growth rate of the deposited films and coatings.

PACS: 52.50.Dg,52.80 Vp

INTRODUCTION

The plasma flows generation of various solid-state materials without the drops of working substance and with the large fraction of ions is the important task from the point of view of their possible practical use. In particular, for the formation of protective coatings, functional layers in micro- and nan-electronics, the development and improvement of metal ion sources, the solution of some problems of working with spent nuclear materials and other tasks of nuclear energy [1, 2]. The non-self-sustained arc discharge in vapors of the anode material are capable to generating of plasma flows with precisely these properties. It is capable to generating the plasma flows of solid-phase materials without drops of the working substance and ensuring even in the non-magnetic versions the part of ions in the generated flows up to 15…20% [3-6]. The non-self-sustained arc discharge in vapors of the anode electrode material in an external magnetic field allow generating the plasma flows of solid-phase materials with a proportion of ions in the flows up to 100% [7, 8].

The aim of this work was to study the influence of the additional non-self-sustained discharge in E×B fields on the characteristics of the main arc discharge in pure zirconium vapor and on the parameters of the generated plasma flows.

1. EXPERIMENTAL SET-UP

The scheme of the experimental device is shown in Fig. 1. The main non-self-sustained arc discharge in the vapors of the working material 2 is “ignited” between the water-cooled anode 4 and the grounded cathode 1. In these experiments, the working material was single-crystal zirconium. It was located in a graphite crucible 3, installed on the upper surface of the anode 4. The cathode of the discharge was made of a tungsten wire with a diameter of 1 mm and was connected to the power supply through a resistance of 10 Ω. The cathode heated current was usually 60 A.

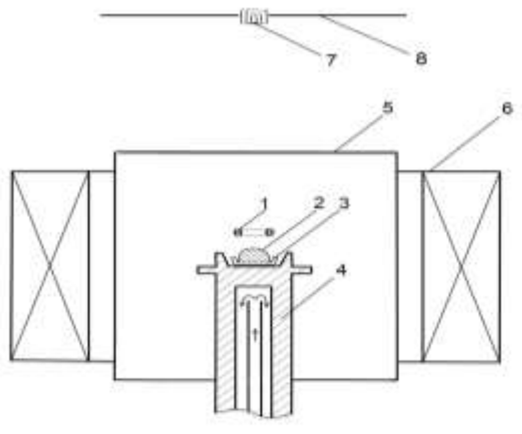

Fig. 1. Experimental device:
1 – heated cathode; 2 – working material; 3 – crucible; 4 – cooled anode; 5 – cylindrical electrode; 6 – magnetic coil; 7 – flat probe; 8 – ion collector

The distance between the discharge cathode 1 and the working material 2 was (0.5…0.7)·10^{-2} m. Magnetic coil 6 was used to create the magnetic field in the discharge gaps of both discharges. In the described experiments, the magnetic field was equal to

$B = 80·10^{-4}$ T. This value of the magnetic field for the discharge in zirconium vapors corresponded to the maximum ion currents on the ion collector 8.

The cylindrical electrode 5 provided the absence of the direct plasma flows of the main arc discharge to the inner surface of the magnetic coil 6. It also served to creates the electric field transverse to the magnetic field and was used also as the anode of the additional electric discharge in the crossed E×B fields between electrode 5 and the cathode of discharge 1. The total ion current in the generated plasma flows was measured by the ion collector 8, which are located at a distance of 0.18 m from anode 4. The ion collector had the negative potential in “-200” V relative to the grounded cathode of the main arc discharge 1. The flat probe 7 with a guard ring was used to study plasma parameters in flows. The recording surface of the probe had the diameter of 4 mm. Under the films deposition the pressure in the vacuum chamber did not exceed $p=2·10^{-3}$ Pa.

The additional gas discharge in crossed electric and magnetic fields between cathode 1 and cylindrical electrode 5 was used to initiate the main arc discharge in vapors of working material 2 between cathode 1 and anode 4 [9]. The additional discharge in pure gas was realized when the positive potential was applied to electrode 5 and the gas was admitted to the vacuum chamber.

The application of a positive potential relative to the grounded discharge cathode 1 to anode 4, at the presence of the additional gas discharge in the crossed fields E×B, led to the formation of a non-self-sustained arc discharge in the gas between this electrodes. The further increase in the current of the non-self-sustained gas discharge lead to the heating of the working material 2 and to the appearance of its vapors in the discharge gap. Under these conditions, the change in the composition of the discharge medium for both discharges is occurred: the transition from discharge in pure gas to the discharge in a mixture of gas with the vapors of the working substance take place. At the definite conditions, when the gas supply to the vacuum chamber was stopped, it was possible to the implement a mode where the working medium of both discharges was only pure vapors of the working material 2.

The additional discharge in the E×B fields in pure zirconium vapors could exist only in the presence of the main arc discharge, when there is no gas flow into the vacuum chamber. From the mode of simultaneous existence of the main arc discharge and the additional discharge in the E×B fields in pure zirconium vapors, it was possible to switch to the mode of existence of only the main arc discharge. This was done by reducing the voltage on the electrode 5 and, accordingly, the current of the additional discharge to zero. Under these conditions, it was possible to ensure the stable existence only of the main arc discharge in pure zirconium vapor.

The initiation of the non-self-sustained vacuum arc discharge in pure zirconium vapors with the help of the additional gas discharge was possible at voltage of the anode power source of the main arc discharge up to 400 V. The initiation of the main arc discharge in the "vacuum diode" mode, even in copper vapors, usually requires the use of power sources with a voltage of more than 1000 V at the initial stage.

2. CHARACTERISTICS OF THE MAIN ARC DISCHARGE IN PURE ZIRCONIUM VAPORS

On the Figs. 2–5 show some characteristics of the main arc discharge in pure zirconium vapors. The characteristics were obtained in the mode of existence only of one main arc discharge, i.e. when the current of the additional discharge in the E×B fields is zero, $I_5=0$.

The volt-ampere characteristic of the arc discharge is presented by curve 1 in Fig. 2. As the given data show, the current-voltage characteristic of this type discharge is “falling”. The increase of the discharge current is accompanied by a decrease in the discharge voltage. Thus, under the conditions of the described experiments, with the increase in the discharge current from $I_d=20$ A to $I_d=40$ A, the discharge voltage are decreased from $U_d=135$ V to $U_d=85$ V. At the same time, the electrical power, which are invested in the main arc discharge are increases.

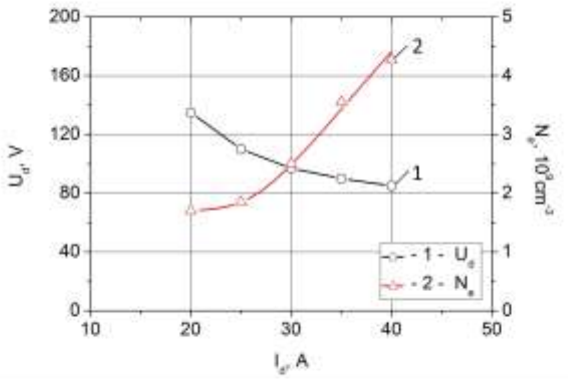

Fig. 2. Dependences of the voltage of the main arc discharge in zirconium vapors U_d and the electron density in plasma flows N_e at different currents of the main arc discharge I_d

The plasma parameters in flows created by main arc discharge in zirconium vapors were obtained using the flat probe with a guard ring. The electron density in the generated plasma streams are shows by the curve 2 of Fig. 2. It can be seen that at the distance of 0.18 m from the anode 4 $N_e \approx (2…4)·10^9$ cm^{-3}. In general, the density of plasma electrons in the flows has a nonlinear dependence on the discharge current. But at discharge currents $I_d \approx 30…40$ A there is something similar to the linear dependence. However, for this statement, additional experimental data at higher discharge currents are needed.

In Fig. 3, curve 1 shows the values of the electron temperature in the generated plasma flows of zirconium vapors at different discharge currents. The data show that at $I_d = 20…40$ A the electron temperature changes slightly and is $T_e \approx 13…14$ eV. That is, it significantly exceeds the value of the first ionization potential of zirconium atoms 6.835 eV.

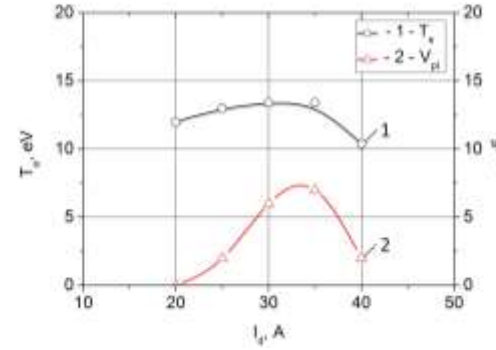

Fig. 3. Electrons temperature T_e and plasma potential V_{pl} in flows of the main arc discharge at different discharge currents I_d

In Fig. 3, curve 2, the values of the plasma potential in the flows are shown. It can be seen that under the experimental conditions the plasma potential is always positive and at the discharge current I_d = 20…40 A is several volts, varying in the range V_{pl} = 0…7 V.

The values of the anode potential drops of the arc discharge at different currents were determined taking into account the values of the plasma potential, Fig. 3, and the strength of the longitudinal electric field in the plasma flows of zirconium vapors, which were obtained in experiments: E ≈ 1.5 V/cm. The results are presented in Fig. 4, curve 1. The given data show that when the voltage on the discharge decreases from U_d=135 V to U_d=85 V, Fig. 2, at the same time, there is a decrease in V_a from 108 to 56 V. According to Fig. 4, curve 3, in the indicated range of discharge currents, the total electrical power of the main arc discharge, $W_d = U_d \times I_d$, steadily increases from 2.7 to 3.4 kW.

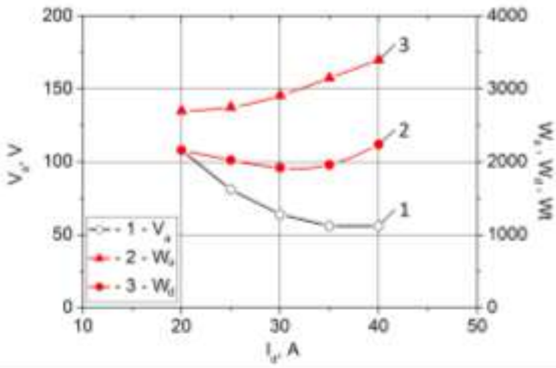

Fig. 4. The anode potential drops of the main arc discharge in zirconium vapors V_a and the electrical power of W_a and W_d at different discharge currents

The electric power which was invested in zone of the anode potential drop of the main arc discharge were estimated in a similar way, $W_a = V_a \times I_d$, and are show in Fig. 4 by curve 2. It can be seen that in the range of discharge currents I_d = 20…30 A, a slightly decrease in W_a is initially observed, which then changes to an increase in W_a at higher discharge currents.

At the same time, the growth rate of deposited zirconium films, q, on the dielectric substrate increases linearly over the entire range of the main arc discharge currents. This is evident from the data of curve 1 in Fig. 5.

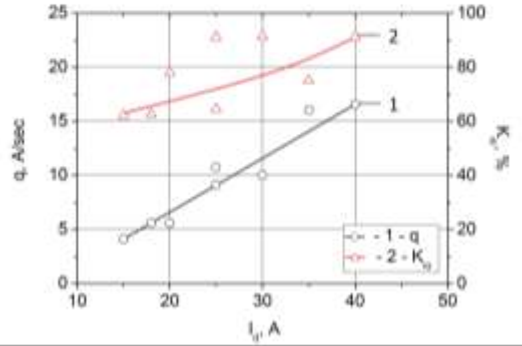

Fig. 5. The growth rates q of the deposited zirconium films and the ionization coefficients of plasma flow K_{io} at different current of main arc discharge I_d and I_5 = 0

The deposition of zirconium films occurred when only the main arc discharge was operating, i. e. at I_5=0, B = $80 \cdot 10^{-4}$ T, and the pressure in the vacuum chamber p = $(1…2) \cdot 10^{-3}$ Pa. The growth rate of the deposited zirconium film were get by the weight method and correspond to the average value q for the entire substrate with a size of $4.8 \times 6 \times 10^{-4}$ m^2. The experimental data show that at the main arc discharge currents in the range I_d = 15…40 A the growth rate of the deposited zirconium films is q ≈ $(5…17) \cdot 10^{-10}$ m/s, or q ≈ 2…6 μm/h.

The calculated values of the ionization coefficient of the zirconium vapors plasma flows K_{io} at different arc discharge currents are presents on the curve 2 of Fig. 5.

The ion component of the plasma flow can significantly affects on the properties of the deposited films during its growth. Therefore, the ionization coefficient is one of the important characteristics of the plasma flow.

The ionization coefficient of the plasma flow, K_i, is defined as the fraction of the ion component in the total plasma flow by the expression:

$$K_i = n_i v_i / (n_i v_i + N_a \times V_a).$$

Here n_i, N_a are the densities of ions and atoms in the flows, and v_i, V_a are the velocities of ions and atoms.

If we assume that only singly ionized ions are present in the plasma flows, the condensation coefficients of ions and atoms in the flows are equal to unity, and there are no processes of self-sputtering and secondary ion-electron emission from the deposited film, then we have the following additional equations:

$$I_{i8o} = e \times n_i v_i \times S_8,$$

$$\Delta m_o = (n_i v_i + N_a \times V_a) \times M_a \times t_{dep} \times S_{sub}.$$

Here I_{i8o} – current to ion collector 8; e – electron charge; S_8 – area of the ion collector 8; Δm_o – mass of the deposited film at this conditions; M_a – mass of an atom of the deposited material; t_{dep} – deposition time; S_{sub} – area of the substrate.

In the absence of self-sputtering of the deposited film and the process of secondary ion-electron emission, for example for conditions of low ion energies, expression for K_i can be written as:

$$K_{io} = I_{i8o} \times M_a \times t_{dep} \times S_{sub} / e \times S_8\ \Delta m_o.$$

This expression makes it possible to determine the real ionization coefficient of K_{io} for the deposited flows, using the values of the ion current to the ion collector 8, I_{i8o}, and the mass of the deposited film Δm_o.

In the presence of the self-sputtering process of the deposited film with a sputtering coefficient S(Ei) there is a decrease in the mass of the deposited film, $\Delta m_s < \Delta m_o$. Therefore, the K_{is} values will be overestimated:

$$K_{is} = I_{i8o} \times M_a \times t_{dep} \times S_{sub} / e \times S_8\ \Delta m_s > K_{io}.$$

The real ionization coefficient can be determined by the formula [8]:

$$K_{io} = K_{is} / (1 + K_{is} \times S(Ei)).$$

When S(Ei)=0 but there is the secondary ion-electron emission from the ion collector with coefficient γ(Ei), the value of the ion current to the collector 8, $I_{i8\gamma}$, will be determined as:

$$I_{i8\gamma} = (n_i v_i + \gamma n_i v_i) \times e \times S_8 = I_{i8o} \times (1+\gamma) > I_{i8o}.$$

The ionization coefficient $K_{i\gamma}$ determined under these conditions will also be overestimated:

$$K_{i\gamma} = I_{i8\gamma} \times M_a \times t_{dep} \times S_{sub} / e \times S_8 \times \Delta m_o > K_{io}.$$

The values of the real coefficient K_{io} at these conditions can be calculated by the expression:

$$K_{io} = K_{i\gamma} / (1 + \gamma\ (Ei)).$$

Here $K_{i\gamma}$ is the calculated ionization coefficient of the plasma flow in the presence of the secondary ion-electron emission process but the absence of the ion sputtering process of the deposited film.

The data shown in Fig. 5 indicate that the ionization coefficient of the generated plasma flows of zirconium vapors at the discharge current I_d = 20 A is about 70%. Its increases with increasing the currents of the main arc discharge up to 90% even at I_5 = 0. These values of K_{io} were calculated taking into account the singly ionized zirconium ions in the flows and the presence of ion sputtering during the films deposition process.

3. THE INFLUENCE OF THE ADDITIONAL DISCHARGE IN E×B FIELDS ON THE CHARACTERISTICS OF THE MAIN ARC DISCHARGE AND PLASMA PARAMETERS IN THE FLOWS

In the described experiments, the additional discharge with ExB fields in pure zirconium vapors was realized only under conditions of stable existence of the non-self-sustained main arc discharge. The main arc discharge between cathode 1 and anode 4, in fact between working materials 2, ensured the presence of working material vapors in the discharge gap. In these experiments it was zirconium. Thus, the plasma flow is formed in the discharge gap between electrodes 1 and 4 and it is propagated in the longitudinal magnetic field of the magnetic coil 6 in the direction of electrode 8. The positive potential applied to cylinder 5 led to the formation of a zone with crossed electric and magnetic fields and the appearance of the additional discharge in the E×B fields between electrodes 1 and 5. The working medium for the additional discharge could be gas, gas and the vapors of zirconium, or the plasma flow of the main arc discharge.

The current-voltage characteristic of the additional discharge in E×B fields are shows on Fig. 6, curve 1.

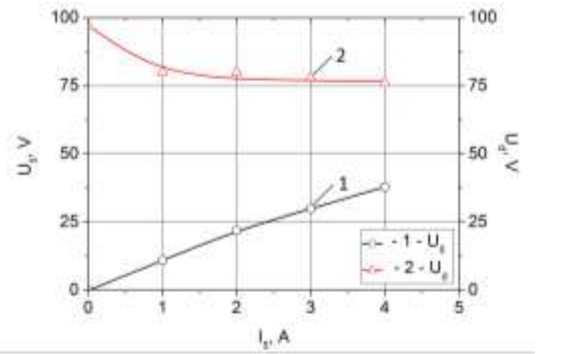

Fig. 6. The voltage of additional discharge U_5 and voltage of main arc discharge in zirconium vapors U_d at different currents of the additional discharge I_5 and I_d=30 A

It can be see that the voltage of the additional discharge does not exceed 50 V at the discharge currents $I_5 \leq 4$ A. Curve 2 in this figure shows the voltage values of the main arc discharge. If there is only one main arc discharge with a current of I_d=30 A, the voltage of the arc discharge is U_d=97 V. The appearance of the additional discharge in the E×B fields leads to a slight gradual decrease of the main discharge voltage up to U_d=76 V at I_5 = 4 A.

At the same time, as shown by the data in Fig. 7, curve 1, the electrical power invested in the additional discharge is $W_5 \leq 150$ W.

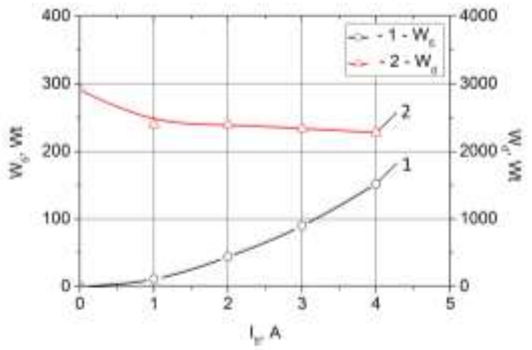

Fig. 7. Dependences the electric powers of the additional discharge W_5 and the main arc discharge W_d on the discharge current I_5 at I_d=30 A

According to curve 2 in Fig. 7, the electrical power invested to the main arc discharge decreases from W_d = 2.9 kW at I_d = 30 A and I_5 = 0 to W_d = 2.3 kW at I_d = 30 A and I_5 = 4 A.

The effect of the additional discharge on the value of the ion current in the generated plasma flows which are fixes the ion collector 8 are shows on Fig. 8, curve 2.

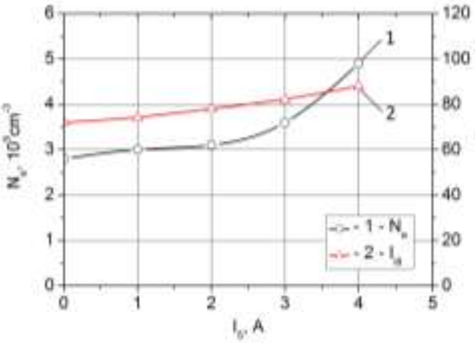

Fig. 8. Dependences of the plasma electron density in the generated flows, N_e, and the ion current to electrode 8 I_{i8} from the additional discharge current I_5 at I_d=30 A

The additional discharge with the current up to $I_5 \leq 4$ A leads to the increase of the ion current from 72 to 82 mA. The simultaneously change in the electron density of the plasma flows are shown by curve 1 of this figure. According to this data, the main arc discharge with a current of I_d = 30 A and I_5 = 0 generates a plasma stream of zirconium vapors with the electron density in the plasma flow $N_e = 2.8 \cdot 10^9$ cm^{-3}.

The additional discharge, even at relatively small discharge currents and small electric power, leads to an increase of the plasma electron density in flows almost 2 times, to $N_e = 4.9 \cdot 10^9$ cm^{-3}. This is show by the data of curve 1 in Fig. 8. The given data are indicate to the expediency of using the additional discharge in E×B fields for increase targeted control of the plasma density in flows generated by both discharges.

The dependences of the ion current on the electrode 8 (curve 1) and the saturation ion current of the flat probe 7 (curve 2) from the plasma density in the created flows are presented on Fig. 9. During these measurements, the probe potential was "-100"V, the current of main arc discharge was constant, I_d = 30 A, but the additional discharge current varied in the range I_5 = 0…4 A.

Similar dependences in the main arc discharge at discharge currents I_d = 20…40 A and at I_5 = 0 indicate a linear increase in the ion current on the collector 8, I_{i8} and the saturation ion current on the flat probe 7, I_{inas}, with the increase of the plasma density in the flows. This allows us to use these parameters to estimate the values of plasma electron density in the main arc discharge flows. However, in the case of simultaneous generation of plasma flows by the main arc discharge and additional discharge, such linear dependences are unfortunately absent.

In the latter case, the linear dependence of the values I_{i8} and I_{inas} on N_e can occur only at $N_e > 3.1 \cdot 10^9$ cm^{-3} or at the currents of additional discharge $I_5 > 2$ A. However, this conclusion needs to the additional confirmation in experiments. The possible explanation of these results can be the fact that at the small currents of the additional discharge there is not only an increase of the plasma density values, but also the expansion of the directional diagram for the plasma flows. That is, at the same time, the redistribution of the ionic component in the flows occurs along to their diameters.

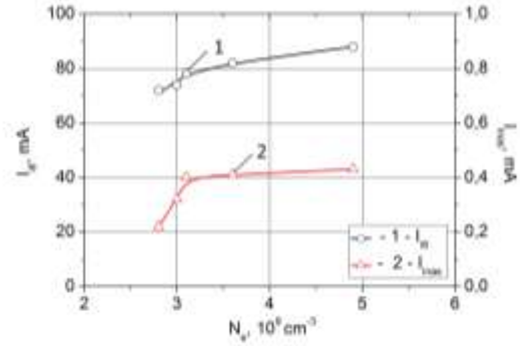

Fig. 9. Dependences of the ion current on electrode 8 I_{i8} and the saturation ion current on the probe 7 I_{inas} from different the plasma electron density in the generated flows. I_d=30 A and I_5 = 0…4 A

The dynamics of electron temperature in the generated plasma flows of zirconium vapors, which is due to the action of the additional discharge, is presented in Fig. 10, curve 1.

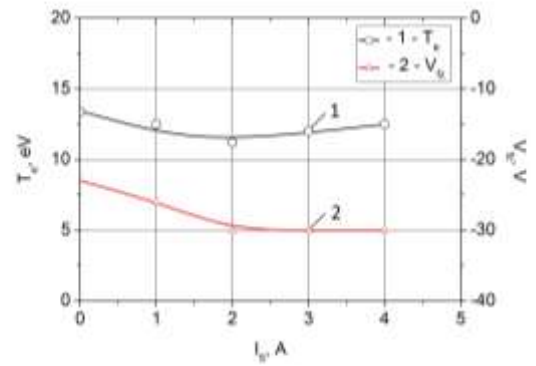

Fig. 10. Dependences of the electrons temperature in plasma flows T_e and the floating potential of the insulated electric probe V_{fz} from the current of the additional discharge I_5 at I_d=30 A

In these measurements, the main arc discharge current was I_d = 30 A and did not change in the entire range of additional discharge currents. It can be seen that the electron temperature is T_e = 11…13 eV in the entire range of the additional discharge currents. It changes slightly when the current I_5 are changes.

The values of the floating potential of the isolated electric probe 7, which was located in the center of the plasma flow at a distance of 0.18 m from the anode of the main arc discharge 4, are shown by curve 2 of Fig. 10. The floating potential of the probe is negative and its value varies from "-23" to "-30 V" in the entire range currents of the additional discharge. That is the volume charge of the created plasma flows is compensated, and these plasma flows can be used to deposit zirconium films and coatings on a substrate of any materials, including a substrate from the dielectric materials.

The values of the plasma potential in the generated flows were determined using the flat electric probe with a protective electrode at different additional discharge currents in E×B fields. This data are presented on Fig. 11, curve 1. It can be seen that the plasma potential in the flows is positive and varies in the interval U_{pl} = +(1…6) eV. Probe measurements performed at different distances from the anode 4 made it possible to estimate the longitudinal intensity of the electric field in the plasma flows approximately as E ≈ 1.5 V/cm. It was also found that the strength of radial electric field in the plasma flow is approximately 0.2…0.3 V/cm and that the electric field is directed towards the center of the plasma flow. The anode potential drop in the main arc discharge was calculated taking into account the experimental values of the longitudinal electric field strength in the plasma flow and the main arc discharge voltage at different current of the additional discharge. The results are presented by curve 2 in Fig. 11 for different additional discharge currents.

It can be seen that the anode potential drop in the near-anode layer of the main arc discharge V_a ≈ 64 V at the arc discharge current I_d = 30 A and I_5 = 0. The anode potential drop decreases in numerical values of V_a, leaving them positive when the additional discharge current changes in the interval I_5 = 0÷4 A.

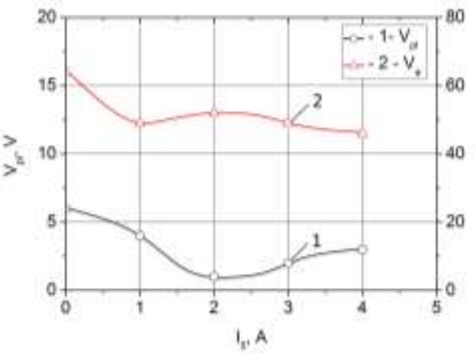

.

Fig. 11. Dependencies of the plasma potential V_{pl} and the calculated anode potential drop V_a for discharges in zirconium vapors from the current of the additional discharge I_5 at I_d = 30 A

The electric power, which are invested into the near-anode layer $W_a = I_d \times V_a$ at various currents of the additional discharge is shown on Fig. 12, curve 1.

The ratio of the electrical power, which are invested in the anode potential drop W_a to the total electrical power of the main arc discharge $W_d = I_d \times U_d$ for different current of the additional discharge I_5 is shown on Fig. 12, curve 2. The results indicate that the ratio Wa/Wd for the main arc discharge in zirconium vapors changes slightly over the entire interval of the additional discharge currents, remaining in the range of values Wa/Wd = 0.65…0.60.

This correlates well with the data presented in Fig. 13. The growth rate of the zirconium films q deposited from the plasma flows of the main arc discharge at current I_d = 25 A and various current of the additional discharge in E×H fields are shown on Fig. 13, curve 1. It can be seen that q remains practically unchanged and is about 9 A/s or q ≈ 3.2 μm/h.

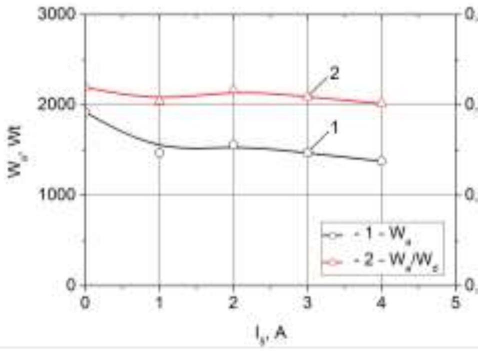

Fig. 12. Electric power invested in the anode potential drop of the main arc discharge $W_a = I_d \times V_a$ and its part in the electric power of the main arc discharge W_a/W_d at different additional discharge currents I_5 and I_d=30 A

Curve 2 Fig. 13 are shows how the additional discharge affects on the ionization coefficient of the generated plasma flows.

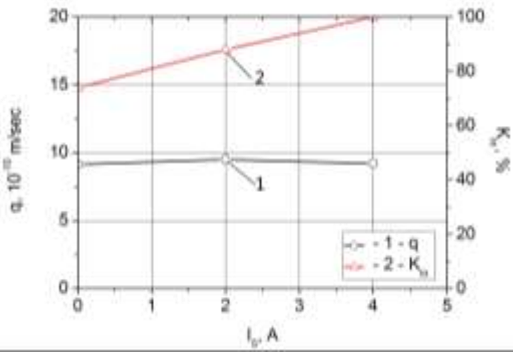

Fig. 13. The growth rate of the film deposited q and the ionization coefficient of the plasma flow K_{io} from the current of the additional discharge I_5 at I_d=25 A

It is clearly seen that the main arc discharge at the current of 25 A is capable of generating the plasma flows with the ionization coefficient K_{io} = 75%. But, the additional discharge is able to increase the part of ions in the total plasma flow up to 100%.

CONCLUSIONS

The paper are presents the results of research of the source of dropless and highly ionized plasma flows of zirconium vapors based on the two-discharge system: the main non-self-sustained arc discharge in anode material vapors with a magnetic field and the non-self-sustained discharge with E×B fields. The main characteristics of these discharges and the plasma parameters of the generated flows were studied.

It is shown that the one arc discharge in the vapors of the anode material under the conditions of the described experiments generates plasma flows of zirconium vapors with a plasma flow ionization coefficient from 60 to 90%. It is established that the additional discharge in E×B fields is capable of increasing the part of ions in the flows from 75 to 100% even at low arc discharge currents.

It has been established that the additional discharge in E×B fields can significantly change the ionization coefficient of the plasma flow without changing the growth rate of the deposited zirconium films. This makes it possible to purposefully influence on the properties of films during the deposition process.

It has been shown that this source is capable the providing deposition of zirconium films and coatings on various materials with growth rates of up to 6 μm/h.

It is shown that the additional discharge in E×B fields is capable to increasing the plasma density in the generated flows up to double and more even at small discharge currents.

It has been established that the additional discharge in zirconium vapors leads to a slight decrease in the numerical values of the anode potential drop in the main arc discharge, leaving it positive.

The presented results indicate the relevance and feasibility of further research into discharges of this type in various working mediums in order to develop new and improve existing plasma technologies.

REFERENCES

1. *Handbook of Plasma Immersion Ion Implantation and Deposition* / Edited by Andre Anders. John Wiley & Sons, Inc. 2000, p. 444.
2. I.I. Aksenov, V.A. Belous. Protecting coatings on uranium // *East European Journal of Physics*. 2014, v. 1, № 4, p. 4-25.
3. V.A. Saenko. Devices for thermoionic deposition // *Instruments and. Experimental Techniques*. 1985, № 3, p. 509-522.
4. H. Ehrich, B. Hasse, K. Müller, R. Schmidt. The anodic vacuum arc. II. Experimental study of arc plasma // *J. Vac. Sci. Technol.* 1988, A 6, p. 2499-2503. https://doi.org/10.1116/1.575535
5. A.G. Borisenko, A.V. Kravchenko, V.A. Saenko. Magnetless plasma metallizer // *Instruments and Experimental Techniques*. 1992, № 2, p. 257-261.
6. G. Musa, H. Ehrich, M. Mausbach. Studies on thermionic cathode anodic vacuum arcs // *J. Vac. Sci. Technol.* 1994, A 12, p. 2887-2895.
7. A.G. Borisenko, V.A. Saenko. The non-self-sustaining arc discharge in anode material vapor as a source of a technological plasma flow // *Trans. of Ukrainian Vacuum Society*. 1995, v. 1, p. 106-109.
8. A.G. Borisenko, V.A. Saenko, V.A. Rudnitsky. Non-self-sustained Arc Discharge in Anode Material Vapors // *IEEE Transactions on Plasma Science.* 1999, v. 27, № 4, p. 877-881.
9. A.G. Borisenko, V.A. Saenko, V.A. Rudnitsky. A Method of Gas Admission for Initiating a Discharge in Anode Material Vapors // *Instrument and Experimental Techniques.* 1999, v. 42, № 2, p. 270-272.

Article received 10.12.2024
Article accepted 16.01.2025

НЕСАМОСТІЙНИЙ ДУГОВИЙ РОЗРЯД У МАГНІТНОМУ ПОЛІ: ВПЛИВ ДОДАТКОВОГО РОЗРЯДУ В E×B-ПОЛЯХ НА ОСНОВНІ ХАРАКТЕРИСТИКИ ДУГОВОГО РОЗРЯДУ В ПАРАХ ЦИРКОНІЮ ТА НА ПАРАМЕТРИ ГЕНЕРОВАНИХ ПЛАЗМОВИХ ПОТОКІВ

А.Г. Борисенко

Представлено результати досліджень несамостійного дугового розряду з магнітним полем у парах цирконію та додаткового несамостійного розряду в E×B-полях. Наведено основні характеристики розрядів. Показано вплив додаткового розряду на електронну температуру, електронну густину плазми, потенціал плазми та плаваючий потенціал у генерованих плазмових потоках парів цирконію. Встановлено, що навіть при малих електричних потужностях додатковий розряд здатний майже вдвічі збільшити щільність електронів плазми в потоках. Показано, що прианодне падіння потенціалу в дуговому розряді має позитивне значення у всьому інтервалі розрядних струмів і зменшується зі збільшенням струму розряду. Показано, що дуговий розряд у парах матеріалу анода здатний генерувати плазмові потоки парів цирконію з коефіцієнтом іонізації від 60 до 90%. Встановлено, що додатковий розряд у полях E×B здатний збільшити частку іонів у потоках від 75 до 100% навіть при малих струмах дугового розряду та може бути використаний для її цілеспрямованого регулювання без зміни швидкості росту нанесення плівок та покриттів.